CRACK TRAJECTORIES DURING FRACTURE OF ANCHORS IN ROCK

A. Fathy*, J. Planas*, J. LLorca*, M. Elices* and G. V. Guinea*

This paper analyzes from the numerical and experimental point of view the crack trajectories during fracture of a plane stress anchor in a quasi-brittle material. The experimental work was carried out on granite anchor plates, where various sizes and loading spans were tested. The crack paths were simulated numerically using linear elastic fracture mechanics (LEFM). For this type of geometry, both LEFM computations and experimental measurements indicate that failure tends to be through a single bilateral crack roughly perpendicular to the load axis. The failure mechanism of this slender two dimensional 2D model is never conical, and extrapolation to 3D axisymmetric pull-out tests is useless. Numerical analyses based on LEFM are able to predict crack trajectories provided that the boundary conditions -which turn out to be nonlinear- are properly stated.

INTRODUCTION

The analysis of the fracture behaviour of anchor bolts embedded in concrete and rock has received great attention in the last decade, as is shown by the RILEM activity in this field (RILEM, 1990; 1991). In this paper, an experimental study and an initial numerical analysis are presented in the case of a plane stress geometry for a steel anchor bolt in a granite plate. Several sizes with different supporting distances were tested and analyzed. The effect of the boundary conditions on the crack trajectories is emphasized here, whereas the application of fracture mechanics techniques to predict the rupture loads was considered in a previous publication (Fathy, 1992; Fathy *et al.*, 1992)

EXPERIMENTAL WORK

The geometry of the plane-stress problem given by RILEM is depicted in Fig. 1. Pull-out test specimens were scaled up to three anchor depths d= 30, 50, and 75 mm, and three loading spans were investigated, corresponding to a=$d/2$, d, and $2d$. Rectangular plates were cut using a water-cooled diamond saw from a single commercial granite plate 30 mm thick. To avoid bias due to potential material anisotropy, the orientation of the specimens was always the same. Three specimens were fabricated for each size and geometry, giving a total of 27 specimens. The anchor opening (T shape) was made using a water-jet cutting system which resulted in a good precise opening of very high

* Departament of Materials Science. Polytechnic University of Madrid. ETS Ingenieros de Caminos. Ciudad Universitaria. 28040 - Madrid, Spain.

accuracy (±0.15 mm). Granite plates were machined to leave a 0.5 mm gap opening to facilitate housing process of anchors. The anchor bolts were made of steel, with a yield limit of 325 MPa.

The test set-up was carefully designed to give clear boundary conditions so as to help in numerical analysis modelling. The load bearing parts of the system (rollers, bearing plates) were scaled in accordance with specimen depth d to preserve geometrical similarity. All tests were performed in a hydraulic testing machine equipped with a 25 kN capacity load-cell of better than 50 N precision. The tests were performed in actuator position control, at a constant displacement rate proportional to the anchor bolt depth d, and the rate was chosen to reach the maximum load 3 to 5 minutes after test initiation. The crack paths were digitized on the broken specimens by means of an image analysis system. More details about the experimental procedure are given elsewhere (3).

NUMERICAL ANALYSES

The first approach to modelling the fracture of granite plates was made using LEFM. The simulation was conducted using the finite element code FRANC (FRacture ANalysis Code). Crack propagation was carried out at constant K_I=K_{Ic}, K_{Ic} being equal to 2.6 MPam$^{1/2}$ for this material (4). To allow LEFM calculations, a short initial crack ($\Delta a \approx 0.02d$) was introduced at the lower corner of the anchor housing in such a direction as to give zero mode II stress intensity factor (more precisely, $K_{II} \leq \pm 0.01 K_{Ic}$). As the crack propagated, the mesh was automatically rebuilt along the crack, leaving element dimensions at the crack tip unchanged. A maximum circumferential stress criterion was used to decide the cracking direction, and the increment in crack length was selected in such a way that the new crack tip was in pure mode I, $K_{II} = 0$, within the limits $K_{II} \leq \pm 0.03 K_{Ic}$.

The geometry and dimensions of the analyzed specimens were exactly the same as those used in the experimental tests. The elastic properties of the granite were E= 39 GPa and ν= 0.2 (3). The steel support and the anchor bolt were modelled with E = 200 GPa and ν = 0.3.

Only half of the specimen was modelled by finite elements. The anchor was modelled in the same way and was separated from the specimen by a 0.5 mm gap except on the load transmitting area, where perfect adhesion was assumed as dictated by the RILEM description of the numerical round robin. The finite element mesh for all specimens is composed of eight-node quadrilateral elements at the initial propagation region and six-node triangular elements elsewhere. The system was loaded by a uniform stress at the end of the anchor shaft .

RESULTS

The crack patterns for the final failure of the various specimens are shown in Figs. 2a to 2c where the drawing scale is inversely proportional to the specimen width ($2.3d + 2a$). In these figures the individual crack paths are shown as thin lines, and in general are seen to start at the lower corner point under the anchor head, propagate downwards (towards the supports), and then rise and grow towards the lateral free boundary of the specimen. In a few cases a strongly non-symmetric failure occurred and the cracks grew down to the supports.

The envelope of the dominant patterns (those not running down to the support) is shown as the shadowed region A in the figures, and is seen to be fairly symmetric, although a very slight asymmetry may anyway be appreciated. The envelope of the few cracks that ran to the supports is the shadowed area B (not present in specimens with $a=d/2$), and corresponds to totally asymmetric fractures.

The numerical crack paths corresponding to LEFM prediction are represented in these figures as a thick line which is symmetric because of the symmetry enforced by the finite element modelization. The essential point is that the LEFM patterns are quite close to the average crack pattern for the dominant (quasi-symmetric) mode for the geometries corresponding to $a=d/2$ and $a=d$, but run quite far from that of the last geometry, the one with $a=2d$.

This divergence of actual and predicted crack paths for the case $a=2d$ was intriguing, and further numerical analyses were performed to investigate the underlying mechanisms. It was suspected that these deviations could be due to the differences between the actual and the assumed interface conditions. Indeed, the assumed contact conditions correspond to perfect adherence, which implies infinite friction, and very small horizontal and rotational movement on the contact area, because of the high relative stiffness of the steel. In reality, there is no adherence, but some kind of frictional contact. Thus a frictional force will act at the beginning of the loading, and when the horizontal movement closes the gap between the plate and the steel shaft, the loading will proceed at a nearly fixed horizontal displacement.

Preliminary computations were performed to study the influence on the crack trajectory of two extreme boundary conditions, namely free horizontal movement and fully constrained movement. The results of such computations are shown in Fig. 3. It appears that when no horizontal kinematic restriction exists, the crack path tends to propagate at approximately 45 ^{0} right to the bottom free boundary (path *ob* in Fig. 3). When the horizontal displacements at the anchor head are restricted in any way, however, the path is completely different and grows nearly horizontally towards the lateral free boundary (paths *oc* and *od* in Fig. 3). The experimental paths run between the above extreme cases and it is possible, in principle, to reproduce them by using non-linear mixed boundary conditions.

To see how an intermediate path may be obtained, the above hypothesized behaviour was simulated in the following very rough way: The load of the anchor bolt was concentrated in one node as depicted in Fig. 4. The three cases shown were analyzed in order to get a feeling about the implied error by concentrating the load in a single node. At the beginning of the calculation, a horizontal frictional force $X = 0.3P$ was assumed (constant friction equal to 0.3). The crack was then propagated under this proportional loading until the horizontal gap was exhausted, and then the computation proceeded at fixed horizontal displacement of the loaded node.

The results are shown in Fig. 5 where it becomes apparent that the crack paths for the three cases (Fig. 4) show the same trend except for very short crack lengths (which may be expected from Saint Venant's principle), and that one may indeed obtain intermediate crack paths by assuming an adequate friction coefficient and an initial gap. This fully supports the idea

that the actual crack path is obtained by a mixed mechanism, where for small displacements a frictional force exists, while for larger displacements the gap is exhausted and a horizontal bearing force appears on the granite.

CONCLUSIONS

For a plane stress anchor, both LEFM computations and experimental measurements indicate that failure tends to be through a single bilateral crack roughly perpendicular to the load axis. The failure mechanism of this slender 2D model is never conical and extrapolation to 3D axisymmetric pull-out tests is useless. Numerical analysis based on LEFM is able to predict crack trajectories provided the boundary conditions are properly stated. Experimental crack patterns were numerically reproduced by splitting the process in a frictional initial phase, followed by a fixed displacement phase after the gap between concrete and steel was closed.

ACKNOWLEDGEMENTS

The authors thank Prof. A. Ingraffea for providing the finite element code FRANC to perform the numerical analyses. Financial support for this research was provided by CICYT under grant PB90-0276, and by the Polytechnic University of Madrid under grant A-91 0020 02-31.

REFERENCES

(1) RILEM TC 90-FMA, "Round-Robin Analysis of Anchor Bolts-Invitation", Mater. Struct., Vol. 23,No. 133, p. 78, 1990.

(2) RILEM TC 90-FMA,"Round-Robin Analysis and Tests of Anchor Bolts-Invitation", RILEM News, Vol. 1, 1991.

(3) Fathy, A., Doctoral Thesis, Polytechnic University of Madrid, 1992.

(4) Fathy A., Planas, J., Elices, M., and Guinea, G. V., Anal. Mec. Fract., Vol. 9, pp. 69-74, 1992.

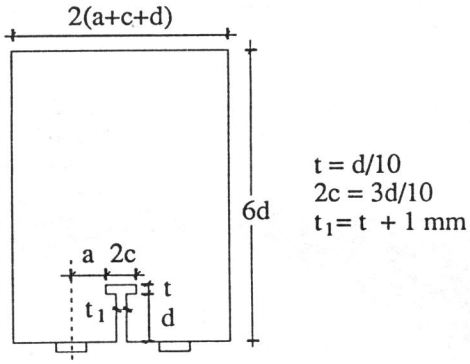

Fig. 1. Specimen geometry.

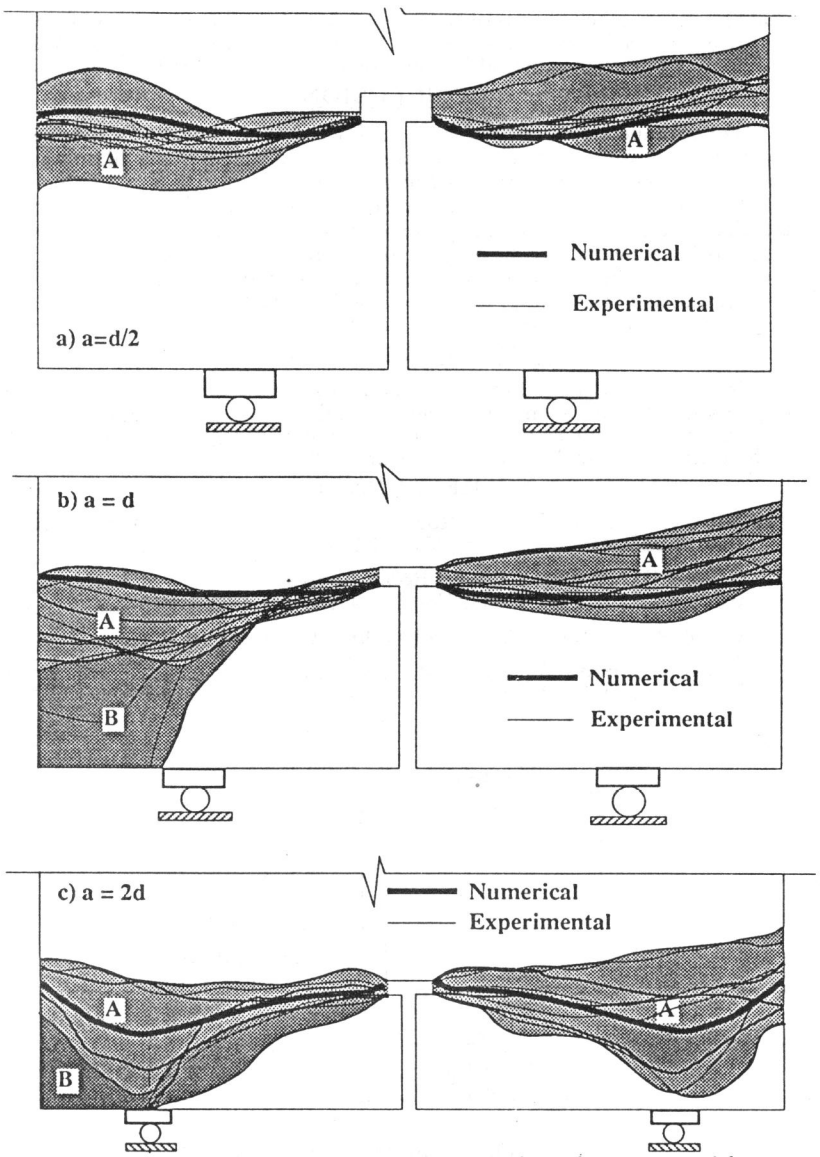

Fig. 2. Comparison of numerically predicted crack patterns with experimental results: a) supports at $a = d/2$, b) supports at $a = d$; c) supports at $a = 2d$.

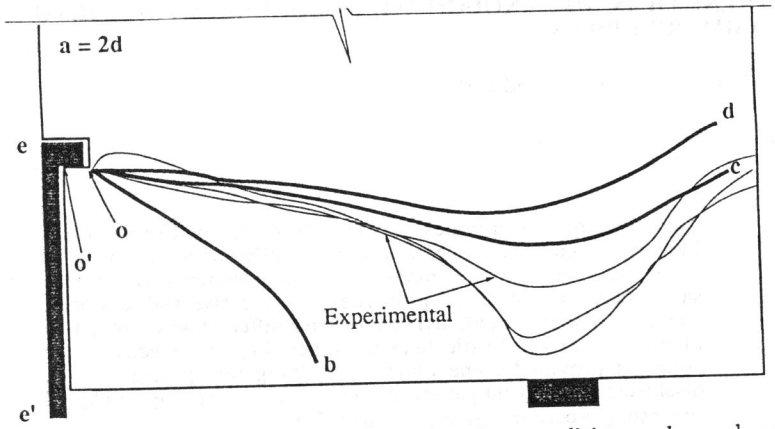

Fig. 3. Crack patterns for various boundary conditions. *ob*: crack path for no horizontal forces. *oc*: crack path for zero horizontal displacement along *oo'*. *od*: crack path for zero horizontal displacement along *ee'*.

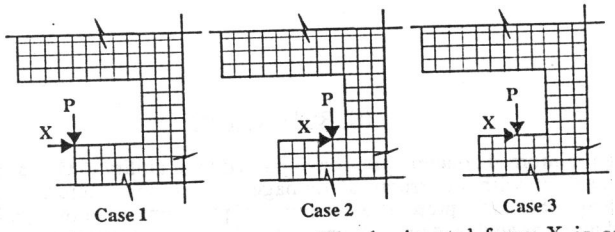

Fig. 4. Simplified loading cases. The horizontal force X is set equal to $0.3P$ (friction coefficient=0.3) until the horizontal displacement fills the initial gap between steel and granite. Subsequent loading proceeds at fixed horizontal displacement at the loaded node.

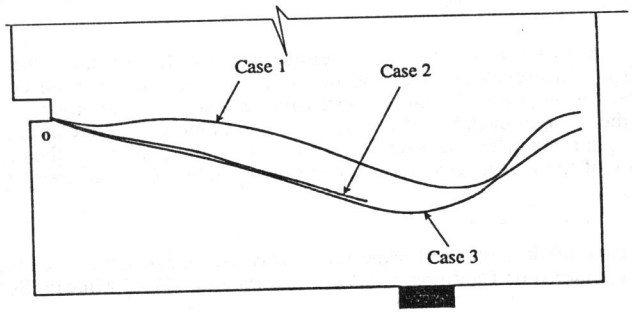

Fig. 5. Crack patterns for the specimens with a=2d. The numerical loading cases correspond to those defined in Fig. 4.